Polyaniline nanofiber supported FeCl$_3$: An efficient and reusable heterogeneous catalyst for the acylation of alcohols and amines with acetic acid

Pravin R. Likhar*, R. Arundhathi, Sutapa Ghosh*, M. Lakshmi Kantam

Inorganic and Physical Chemistry Division, Indian Institute of Chemical Technology, Hyderabad 500670, India

ABSTRACT

An efficient and reusable polyaniline nanofiber supported ferric chloride catalyst was developed and characterized by FT-IR, UV–vis, XPS, TEM and XRD techniques. The catalyst was used in the selective acylation of alcohols and amines employing acetic acid as an acylating agent to obtain the corresponding acetates and acetamides in good to excellent yields.

1. Introduction

Heterogeneous systems have tremendous potential over the homogeneous ones and through heterogenizing the catalyst certain practical limitations of the homogeneous system can be eliminated. The most promising advantages of heterogeneous catalysts are easy separation from the reaction mixture, allowing recovery of the solid and eventually its reuse, provided that the recovered catalyst has not become deactivated during the course of the reaction. The heterogenization can be achieved by the immobilization of the soluble catalyst onto an insoluble matrix usually polymers using a simplified protocol [1–5]. A recent development in the heterogenization techniques includes microencapsulation [6–8] and incarceration [9,10] using polymers to contain the metal complexes inside the polymer wrap *via* π-interaction and physical forces. However, the lengthy procedure and metal leaching are the major limitations in the preparation of polystyrene and polystyrene-derived materials for microencapsulation and incarceration technique. Consequently, the easy synthesis and recycling of heterogenized catalyst with ideal recyclable numbers is a long-term endeavor target.

Among π-conjugate polymers, polyaniline (PANI) is one of the most widely studied conducting polymers for their excellent electronic and optical applications due to its environmental stability and interesting redox properties [11,12]. But only limited appli-

cations are known as PANI-supported metal catalyst in organic transformations [13–17]. We conceived the use of interactive PANI prompted by its highly conducting and redox properties as a support that holds metal complexes securely during catalytic reactions. Furthermore, its easy preparative protocol from non-expensive starting material (aniline), controllable doping levels through an acid doping/base doping process, inert nature and non-solubility in most of the organic solvents and water are impressive qualities for using it as support in heterogeneous catalysis. Herein, we disclose the improved method for the preparation, characterization and evaluation of PANI nanofiber supported FeCl$_3$ (PANI$_n$–Fe) catalyst in acylation of diverse alcohols and amines using acetic acid as an acylating reagent under solvent-free conditions.

The acylation process of alcohols and amines to corresponding acetates and acetamides using acetic acid is both economically and environmentally advantageous. Though the acylation of alcohols and amines can be brought about by the reaction of Lewis acid reagents in conjunction with acetic acid, the Lewis acid is destroyed in the workup procedure resulting in substantial waste production [18,19]. Recently, research has been directed to overcome the above problem which culminated in the development of insoluble solid acids, such as, montmorillonite K10, KF–Al$_2$O$_3$, molecular sieves [20–22], sulphated zirconia [23], zeolites [24], LaY and HY [25,26] as catalysts. Previous reports using clay catalyst still utilizes acetic anhydride as an acylating agent, while metal triflates are soluble and difficult to recover and reuse in the process although acetic acid is used as the acylating agent [27,28]. Therefore, there is a need to develop a reusable and inexpensive heterogeneous catalyst for the

* Corresponding authors. Tel.: +91 40 27193510; fax: +91 40 27160921.
E-mail addresses: plikhar@iict.res.in (P.R. Likhar), sghosh@iict.res (S. Ghosh).

acylation, using acetic acid as acylating agent to achieve high atom economy.

2. Experimental

2.1. Materials and methods

Aniline monomer was distilled under reduced pressure. Other reagents such as ammonium peroxydisulphate and $FeCl_3 \cdot 6H_2O$ were used as received. $FeCl_3 \cdot 6H_2O$ and acetic acid were purchased from s.d. Fine Chemicals, India. All alcohols and amines were purchased from Aldrich or Fluka and were used without further purification. ACME silica gel (60–120 mesh) was used for product purification. All the solvents and chemicals were obtained from commercial sources and purified using standard methods.

Infrared spectra were recorded on a Thermo Nicolet Nexus 670 FT-IR spectrometer as KBr pellets. UV–vis spectra for samples PANI nanofiber in N-methyl pyrrolidinone (NMP) solvent and $PANI_n$–Fe in nitromethane were recorded on a GBC Cintra 10^e UV–vis spectrometer in the range 300–1050 nm with a scan speed of 200 nm/min. X-ray photoelectron spectra were recorded on a KRATOS AXIS 165 with dual anode (Mg and Al) apparatus using the Mg Kα anode. The particle size and external morphology of the samples were observed on a PHILIPS TECNAI F12 FEI transmission electron microscopy (TEM). X-ray powder diffraction (XRD) data were collected on a Simens/D-5000 diffractometer using Cu Kα radiation. Thermogravimetric (TG), differential thermal analysis (DTA) and the mass of the gas evolved during the thermal decomposition of the catalyst were studied on a TGA/SDTA Mettler Toledo 851^e system using open alumina crucible containing samples weighing about 8–10 mg with a linear heating rate of $10\,^\circ C\,min^{-1}$. Nitrogen was used as purge gas for all these measurements. NMR spectra were recorded on a Varian Gemini (200 MHz), a Bruker Avance (300 MHz) or a Varian Unity (400 MHz) spectrometer using TMS as an internal standard and $CDCl_3$ as solvent. Melting points were recorded on a Barnstead electrothermal 9200 instrument and are uncorrected.

2.2. Preparation of $PANI_n$–Fe catalyst

The preparation of PANI nanofiber was achieved by using interfacial method [29]. The polymerization occurred only at the interface of water and toluene where the initiator ammonium peroxydisulphate was in the water phase and monomer aniline was in the organic phase. These PANI nanofibers were rapidly diffuses away from the reactive interface into the water layer.

In a typical procedure, 0.2 mL of aniline monomer was dissolved in 10 mL toluene. Ammonium peroxydisulphate solution (1.0 M) was added to this solution at 0 °C under supersonic stirring condition (for PANI nanofiber, the small portion of precipitate formed was collected by filtration and washed with distilled water until the filtrate became colorless). Further, $FeCl_3 \cdot 6H_2O$ (8.1 g) dissolved in 10 mL of de-ionized water was added drop wise into the above solution over 10 min at room temperature. The quantity of $FeCl_3$ used for the preparation of $PANI_n$–Fe catalyst was optimized using different concentrations of $FeCl_3$ solution based on the higher yields of the acylated product obtained without any leaching of $FeCl_3$ up to five cycles of reaction. Yield of the acylated product obtained remained same at higher concentration of $FeCl_3$ (8.0 wt.% Fe) with considerable leaching of $FeCl_3$.

The doping of $FeCl_3$ into polyaniline nanofiber was achieved by supersonic stirring condition at low temperature to avoid the reduction of ferric chloride. The pH value of the solution before and after adding the solution of $FeCl_3 \cdot 6H_2O$ was ca. 10 and 2, respectively. The solution was stirred for about 12 h. The resulting suspension was separated by centrifugation at 2800 rpm for 5 min and then washed
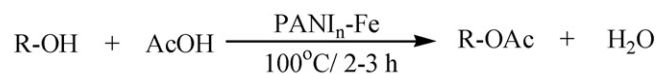
Table 1
XPS data of $FeCl_3$, PANI nanofiber and $PANI_n$–Fe.

XPS peaks	$FeCl_3$	PANI nanofiber	$PANI_n$–Fe
N	–	398.9[a], 400.2[b]	400.0[a], 401.8[b]
Fe 2p$_{3/2}$	713.6, 709.6[c]	–	712.9, 710.0[c]
Fe 2p$_{1/2}$	727.3, 724.9[c]	–	725.7, 723.6[c]

[a] Binding energy of N 1s assigned to –NH–.
[b] Binding energy of N 1s assigned to –N=.
[c] Binding energies of Fe in +2 oxidation state.

$$R\text{-}OH \ + \ AcOH \ \xrightarrow[100\,^\circ C/\,2\text{-}3\,h]{PANI_n\text{-}Fe} \ R\text{-}OAc \ + \ H_2O$$

R= Aralkyl, cyclohexyl

Scheme 1. Acylation of alcohols with acetic acid.

with distilled water several times so as to ensure that no free ferric chloride was present in $PANI_n$–Fe catalyst. Finally, $PANI_n$–Fe catalyst was washed with ethanol and ether three times and then dried under vacuum for 24 h. The iron content in the catalyst was found to be 19.9% by AAS analysis. $PANI_n$–Fe catalyst was fully characterized by FT-IR, UV–vis, XPS (Table 1), TEM and XRD techniques. Similarly PANI–Fe catalyst was prepared following the literature procedure [15] to compare the catalytic activity with $PANI_n$–Fe catalyst. The iron content in the PANI–Fe catalyst was found to be 11% by AAS.
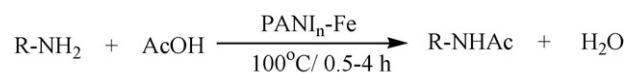
2.3. General procedure for acylation using $PANI_n$–Fe

In a typical acylation procedure, a mixture of substrate (1.5 mmol), acetic acid 2 mL (39.21 mmol) and $PANI_n$–Fe catalyst (25 mg, 5 wt.% Fe) was stirred at 100 °C for an appropriate time as shown in Schemes 1 and 2; Tables 3–5. On completion of the reaction as monitored by TLC, the reaction mixture was cooled to room temperature. Then the catalyst was centrifuged, washed several times with ethyl acetate and the solvent was concentrated under reduced pressure. The crude product was then subjected to a short silica bed and hexane was used to elute the corresponding product in high purity, which does not require any further purification (all the crude acetamides product were purified using hexane/ethyl acetate: 70/30 (v/v) as eluent). All the products were characterized by using NMR and mass spectroscopy and compared with literature data [30,31]. The characterizations of new compounds are given below.

2.3.1. Characterization of the products
2.3.1.1. Acetic acid-4-phenoxy-benzyl ester (Table 3, entry 7). Oily liquid. Yield: 0.207 g (91%); ^{1}H NMR ($CDCl_3$, 200 MHz): δ = 2.18 (s, 3H, CH_3), 7.39 (m, 10H, Ar–H); ^{13}C NMR ($CDCl_3$, 50 MHz): δ = 20.95, 74.42, 126.40, 126.81, 127.48,. 127.92, 128.24, 128.73, 143.07, 143.28, 170.30. Expected Mol. wt.: 242, observed ESI-MS Mol. wt. (M+Na): 265. CHN analysis for $C_{15}H_{14}O_3$ (Calcd.): C, 74.36; H, 5.82. Found: C, 74.42; H, 5.79.

2.3.1.2. Acetic acid-4-nitro-benzyl ester (Table 3, entry 14). White solid. M.P. 65–67 °C. Yield: 0.210 g (85%); ^{1}H NMR ($CDCl_3$, 200 MHz): δ = 2.14 (s, 3H, CH_3), 5.18 (s, 2H, CH_2), 7.52 (d, J = 9.06 Hz, 2H, Ar–H), 8.29 (d, J = 9.06 Hz, 2H, Ar–H); ^{13}C NMR ($CDCl_3$, 50 MHz):

$$R\text{-}NH_2 \ + \ AcOH \ \xrightarrow[100\,^\circ C/\,0.5\text{-}4\,h]{PANI_n\text{-}Fe} \ R\text{-}NHAc \ + \ H_2O$$

R= Ar, aralkyl, heterocylic, cyclohexyl

Scheme 2. Acylation of amines with acetic acid.

$\delta = 20.83, 64.76, 99.99, 128.38, 170.30$. Expected Mol. wt.: 195, ESI-MS observed Mol. wt. (M+Na): 218. CHN analysis for $C_9H_9NO_4$ (Calcd.): C, 55.39; H, 4.65; N, 7.18. Found: C, 55.32; H, 4.61; N, 7.11.

3. Results and discussion

3.1. Characterization of PANI$_n$–Fe

In the preparation of polyaniline nanofiber supported FeCl$_3$ catalyst, it was observed that ferric chloride acts as a Lewis acid as well as weak oxidizing agent, thereby, resulting as a redox reaction assisted by Lewis acid–base process. The preparation of polyaniline nanofiber is the crucial step, which affects the preparation and catalytic activity of PANI$_n$–Fe catalyst. We observed that the preparation of polyaniline in the form of nanofiber could be achieved by controlled addition of oxidant to the aniline at 0 °C and water dilution immediately. The polyaniline nanofiber formed at an early stage in the polymerization process has high surface area, high conductivity and average diameter 30–35 nm. The addition of excess oxidant to the reaction resulted in the secondary growth of polyaniline and finally into an irregular shaped agglomerates of nanofiber and particulates. The PANI$_n$–Fe catalyst was well characterized using FT-IR, UV–vis, XPS, TEM, XRD and TGA/DTA.

3.1.1. FT-IR spectroscopy

The characteristic vibrational absorbance of PANI$_n$ and PANI$_n$–Fe are shown in Fig. 1. The most important band in the spectrum of PANI$_n$ are appeared at 1565, 1494, 1388, 1306, 1194, and 778 cm^{-1} and are attributed to the stretching vibration of amines moiety (quinoid, $\nu_{C=N} + \nu_{C=C}$), imines moiety (benzenoid, $\nu_{C=C}$) units of the polymers, deformations of the C–N bond, stretching vibrations of the C–N bond, in-plane deformations of C–H bonds present in the aromatic rings of the undoped polymers and the out of plane deformations of C–H bonds in 1,4-substituted aromatic ring, respectively [32,33].

The shift of quinoid and benzenoid units of the polymers after doping with metal salt depends on the nature of metal ions. The characteristic peak for benzenoid at 1565 cm^{-1} red shifted 1581 cm^{-1} indicating the weakening of N=Q=N bond. Similarly peak for quinoid at 1494 cm^{-1} shifted to 1503 cm^{-1}. In PANI$_n$–Fe,
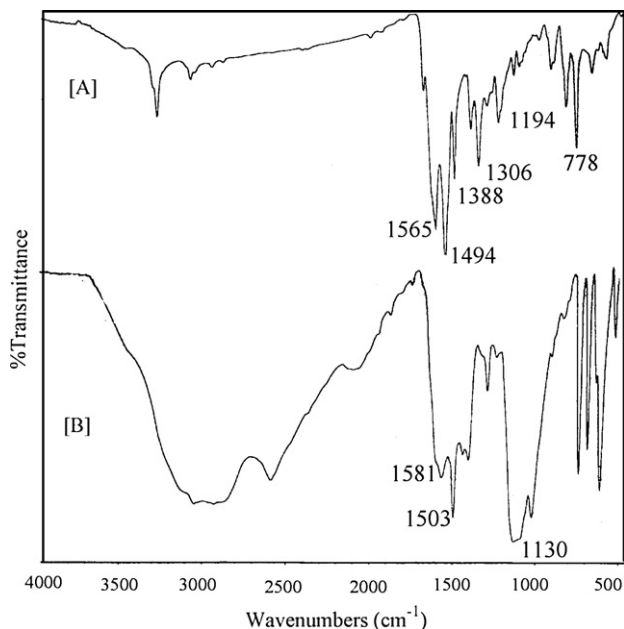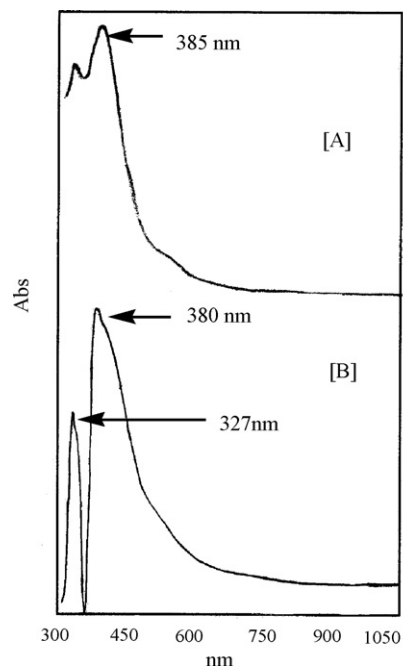

Fig. 2. UV–vis spectra of [A] PANI nanofiber and [B] PANI$_n$–Fe.

a strong new peak at 1130 cm^{-1} was observed for the charged polyaniline chain (C–H$_{in-plane}$ bending).

3.1.2. UV–vis-DRS spectroscopy

Fig. 2 depicts the UV–Vis absorption spectra of PANI nanofiber and PANI$_n$–Fe in *N*-methyl pyrrolidine and nitromethane solution, respectively. PANI nanofiber solution exhibits the absorption peak (λ_{max}) due to π–π^* absorption at 385 nm and PANI$_n$–Fe solution shows absorbance at 380, 327 nm. The absorbance at 380 nm is comparable to those of PANI nanofiber but it is shifted slightly to a shorter wavelength. Polyaniline chain with metal complexation has less extended π-electron delocalization, therefore, has shorter π-conjugation length. The absorbance peak at 327 nm observed for the interaction of ferric chloride with PANI nanofiber.

3.1.3. X-ray photoelectron spectroscopy

The XPS survey scan of PANI$_n$–Fe shows the presence of nitrogen (400.0 eV) and iron (712.9 eV) as illustrated in Table 1. High resolution narrow scan of PANI$_n$–Fe shows binding energy peaks at 712.9 and 725.7 eV corresponding to Fe 2p$_{3/2}$ and Fe 2p$_{1/2}$, respectively. These peaks could be deconvoluted into two peaks each, i.e., 710.0 and 712.9 eV due to Fe 2p$_{3/2}$ and 723.6 and 725.7 eV due to Fe 2p$_{1/2}$. The binding energy peaks at 710.0 eV (Fe 2p$_{3/2}$) and 723.6 eV (Fe 2p$_{1/2}$) are characteristic of Fe in +2 oxidation state whereas, the binding energy peaks at 712.9 eV (Fe 2p$_{3/2}$) and 725.7 eV (Fe 2p$_{1/2}$) are attributed to Fe in +3 oxidation state. The binding energy peaks observed for N 1s at 400.0 and 401.8 eV are assigned due to –NH– and –N=, respectively [34]. The XPS data of PANI$_n$–Fe supports the fact that FeCl$_3$ acts as a weak oxidizing agent to oxidize emeraldine PANI$_n$, which further assists in the Lewis acid–base process. This can be visualized by XPS analysis where changes in the intensity of the peaks due to Fe (III) state and N in the form of amine and imine are observed (Figs. 3 and 4). The binding energy peaks of FeCl$_3$ before doping appeared at 713.6 and 727.3 eV for Fe (III) state correspond to Fe 2p$_{3/2}$ and Fe 2p$_{1/2}$ photoelectron transitions, respectively. The increase in the intensity of binding energy peak at 710.0 eV (Fe 2p$_{3/2}$) due to Fe^{2+} in PANI$_n$–Fe catalyst, clearly suggests that there is reduction of Fe(III) to Fe(II) when FeCl$_3$ is supported onto PANI$_n$. The observed changes in the intensities of the binding
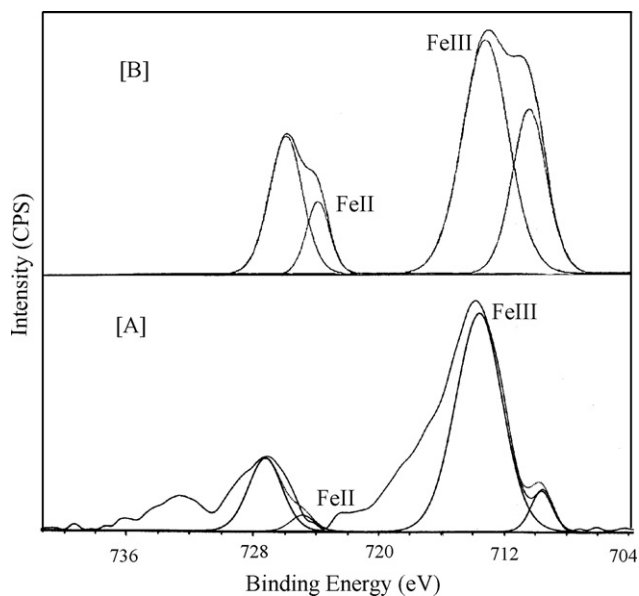

Fig. 1. FT-IR spectra of [A] PANI nanofiber and [B] PANI$_n$–Fe.

Fig. 3. XPS spectra of [A] FeCl$_3$·6H$_2$O and [B] PANI$_n$–Fe. Change in population of Fe (III) and Fe (II) state after doping.

Fig. 4. XPS spectra of [A] N 1s state of PANI nanofiber and [B] N 1s state of PANI$_n$–Fe (after FeCl$_3$·6H$_2$O doping). Change in N 1s state of amine and imine nitrogen.

energy peaks of amine and imine in N 1s is in consonance with the observations made in the binding energy peak of Fe in 3+ oxidation state. The reduction of Fe (III) state reflects the similar change in N 1s signal from polyaniline to PANI$_n$–Fe. Therefore, we postulate that the majority of the dopant molecules interact with the polymer matrix *via* Lewis acid–base complexation with the existence
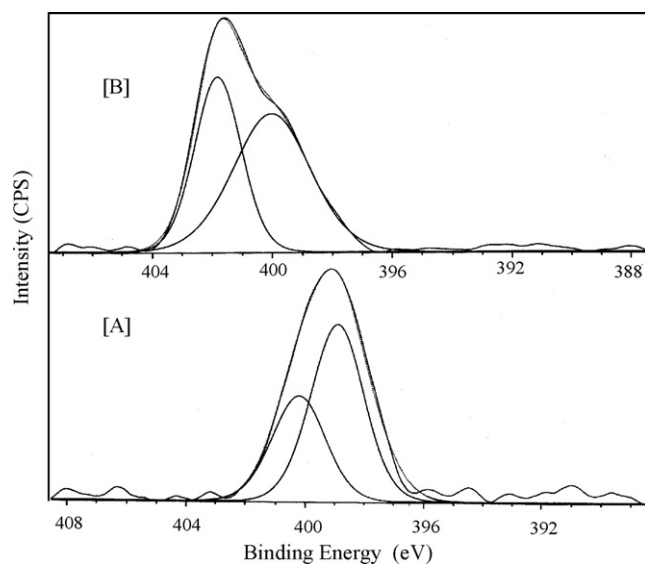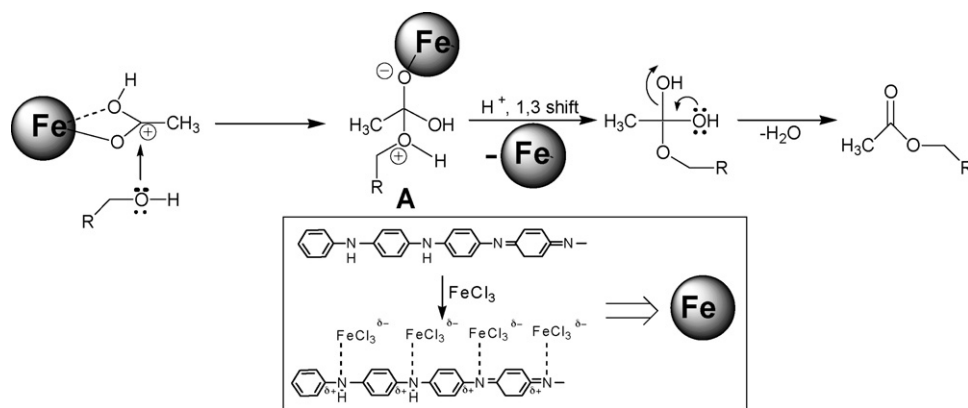
of small fraction, which participates in redox reaction involving the oxidation of reduced fragments of polyaniline. The probable structure is shown in Scheme 3.

3.1.4. TEM

Fig. 5 shows a transmission electron micrograph (TEM) of a polyaniline nanofiber and PANI$_n$–Fe. Individual nanofiber can be

Scheme 3. Complexation of FeCl$_3$ with two different coordination sites and possible role of PANI$_n$–Fe in the acylation reaction.

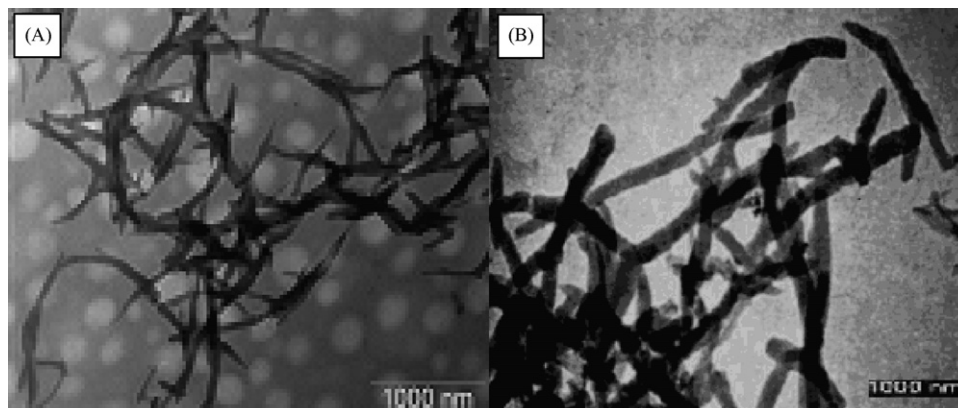**Fig. 5.** TEM images of [A] polyaniline nanofiber and [B] PANI$_n$–Fe.
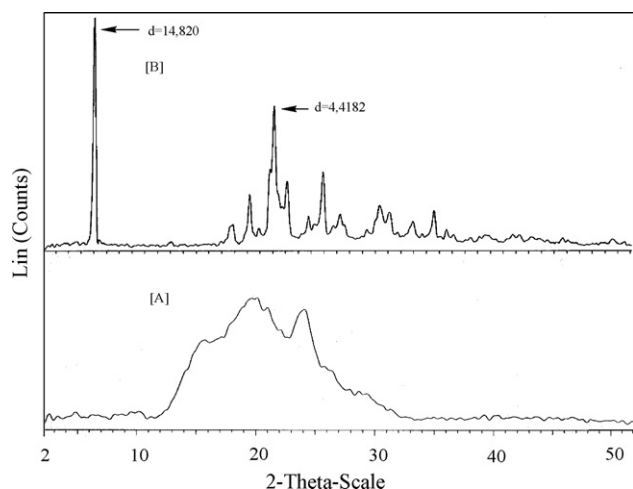
Fig. 6. XRD spectra for [A] PANI nanofiber and [B] PANI$_n$–Fe.

Table 2
Optimization of reaction conditions for the acylation of benzyl alcohol with acetic acid using PANI$_n$–Fe[a].

Entry	X (wt.%)	Temperature (°C)	Solvent	Time (h)	Isolated yield (%)
1	2.5	100	–	3	32
2	5	100	–	2.5	86
3	8	100	–	2.5	87
4[b]	5	80	CH$_3$CN	3	41
5[c]	5	Reflux	CH$_2$Cl$_2$	25	72

[a] Alcohol (1.5 mmol), acetic acid 2 mL (39.21 mmol), and PANI$_n$–Fe (X wt.%).
[b] Using acetic acid (1.1 equiv.) and CH$_3$CN (3 mL).
[c] Using acetic acid (1.1 equiv.) and CH$_2$Cl$_2$ (5 mL).

discerned along with regions of metal salt (the darker images). The diameters and lengths of nanofiber were found to be in the ranges of 30–35 and 200–300 nm, respectively before doping. Since there was excess metal salt in the solution, we believed that the metal salt also penetrated within the individual nanofiber. The TEM photographs suggested that, the surface morphology and size of fibers were transformed into relatively thick fibers after doping with FeCl$_3$. It was also clear from the TEM-images that all of the nanofiber had a uniform fibrous morphology before and after doping with FeCl$_3$.

3.1.5. XRD

The powder XRD patterns of PANI nanofiber and PANI$_n$–Fe catalyst were shown in Fig. 6. The XRD pattern of PANI nanofiber was similar to that of particulate of PANI [29] and the intensity of amorphous peak at 2θ was found to be 20°. In XRD pattern of PANI$_n$–Fe, we found that FeCl$_3$ doping caused the alteration in d-spacing and 2θ value indicated the interaction of FeCl$_3$ with the surface of polyaniline nanofiber. The calculated crystalline size [nm] of PANI$_n$–Fe for 1st peak was found to be 26.5 and for 2nd peak was found to be 11.2 based on observed d-spacing values 14.820 and 4.4118 and observed 2θ values 6 and 20.1, respectively.

The thermal behavior of PANI nanofiber and PANI$_n$–Fe was investigated by TGA instrument at the heating rate of 10 °C/min in air. PANI nanofiber were stable upto 111 °C while PANI$_n$–Fe was stable up to 135 °C indicated the increase in stability of PANI$_n$–Fe after complexing with FeCl$_3$.

As mentioned in the experimental part, during the addition of aqueous solution of ammonium peroxydisulphate (APS) to the aniline solution, aniline micelles were formed in the medium and simultaneously the aqueous solution of FeCl$_3$ was added in the solution. Thus Fe^{3+} ions also participated in the formation of aniline micelles because amphiphilic nature of aniline (presence of hydrophobic benzene ring and hydrophilic amine group). The above described micelles are regarded as the "soft-templates". The oxidation polymerization of aniline was influenced by the hydrophilic nature of FeCl$_3$, a mild oxidant at the micelle/water interface and the growth of the nanofibers was allowed by an accretion [35] or elongation process [36]. In general, the accretion or elongation process is mainly controlled by the redox potential of the oxidant. The redox potential of FeCl$_3$ is about 0.76, which is much lower than that of APS [37]. Thus, the diameter of the composite nanofibers is smaller if prepared in the presence of FeCl$_3$, rather than oxidized by APS alone. The composite nanofibers oxidized by APS and FeCl$_3$ show smaller diameter, higher crystallinity, higher stability and high conductivity. The excess FeCl$_3$ acted as dopant for the highly conducting nanofibers and adsorbed on the nanofibers by ionic interaction and finally the diameter of the nanofibers were increased (as observed in TEM images). Subsequently, it was found that the composite PANI$_n$–Fe is most stable, highly active and reproducible catalyst compared to PANI–Fe [15] which has lower surface area resulted into lower catalyst loading, lower catalytic activity and less stable nanocomposite. Thus considerable leaching of FeCl$_3$ was observed in PANI–Fe catalyst.

3.2. Application of PANI$_n$–Fe in acylation reaction

We have studied the effect of Fe loading on the acylation of benzyl alcohol with acetic acid in neat acetic acid and subsequent work was focused on optimization of various reaction parameters such as temperature, time and different solvent systems such as acetonitrile and dichloromethane (Table 2). It was observed that, 5 wt.% of Fe afforded acylated product in high yield without leaching of Fe (Table 2, entry 2). To examine the effective role of acylating reagent using 1 equiv. amount in the acylation reaction of alcohols and amines [38–43], we used 1.1 equiv. of acetic acid in dichloromethane (5 mL) under same optimized reaction condition. It was observed that, the reaction was smooth and gave good yields but the reaction took prolonged time for completion (Table 2, entry 5). To study the applicability, stability and scope of PANI$_n$–Fe catalyst for the acylation reactions, a wide range of structurally and electronically varied alcohols (1.5 mmol) were subjected to react with acetic acid (2 mL, 39.21 mmol) using 25 mg of PANI$_n$–Fe at 100 °C to afford corresponding acetates in good to excellent yields (Scheme 1). The results are summarized in Table 3. Various electron-rich, sterically hindered benzyl alcohols underwent reaction with acetic acid at 100 °C for 2–3.5 h to afford the corresponding acylated products in high yields (Table 3, entries 1–7). Alkylthio substituted benzyl alcohol also afforded the corresponding O-acylated derivatives in good yield when treated with acetic acid (Table 3, entry 8). Acylation of phenolic hydroxy group could not be facilitated under similar conditions whereas selective acylation was observed with alcoholic hydroxy group (Table 3, entry 9). Similarly in presence of donating group, the alcoholic hydroxy group was acylated selectively in shorter reaction time (Table 3, entry 10). The excellent 'electrophilic activation' was observed for alcohols having electron withdrawing groups that decrease the nucleophilic property of the hydroxyl group (Table 3, entries 11–14). In case of long chain alcohols, 2-phenylethanol, the acylation was found at a relatively faster rate with high yield (Table 3, entry 15).

It was observed that primary alcohols undergo acylation at a shorter period of time compared to secondary alcohols. It is important to note that in acylation of both primary and secondary alcohols, there was no by-product formation observed. Secondary alcohols when subjected to reaction with acetic acid the corresponding O-acylated products were obtained in high yields and the results are summarized in Table 4. Sterically hindered diphenyl methanol, cinnamyl alcohol and cyclohexanol also gave the acylated products in high yields (Table 4, entries 3–5).

Table 3
Acylation of benzyl alcohols with acetic acid using PANI$_n$–Fe[a].

Entry	Alcohol	Product	Time (h)	Isolated yield (%)
1			2.5,12	86
2			2.0	77
3			2.0	83
4			2.5	91
5			2.5	84
6			2.5	92
7			2.0	91, 94[b], 83[c]
8			3.0	63
9			3.5	85
10			2.5	71
11			3.0	87
12			2.5	92
13			3.0	56
14			2.0	85
15			2.0	88

[a] Alcohol (1.5 mmol), acetic acid 2 mL (39.21 mmol) and catalyst 25 mg at 100 °C.
[b] Yields using an FeCl$_3$ catalyst (162 mg, 1.0 mmol).
[c] Yields using PANI–Fe (50 mg).

Table 4
Acylation of secondary alcohols with acetic acid using PANI$_n$–Fe[a].

Entry	Alcohol	Product	Time (h)	Isolated yield (%)
1			1.5	86
2			2.0	77
3			1.5	72
4			0.5	95, 98[b], 77[c]
5			2.5	67

[a] Alcohol 1.5 mmol, acetic acid 2 mL (39.21 mmol) and catalyst 25 mg at 100 °C.
[b] Yield using an FeCl$_3$ catalyst (162 mg, 1.0 mmol).
[c] Yield using PANI–Fe catalyst (50 mg).

position of aniline affects the nucleophilicity and steric hindrance, respectively and thus, the corresponding products are obtained in low yields (Table 5, entries 7 and 8). Heterocyclic amine and cyclohexyl amine with acetic acid also gave the corresponding product in moderate yields (Table 5, entries 9 and 10). Benzyl amine, substituted benzyl amines and 2-phenethyl amine underwent reaction with acetic acid and the corresponding acetamides were obtained in good yields (Table 5, entries 11–15). In case of 2-aminophenol and 4-aminophenol, only amine group was selectively acylated to form 2-acetamidophenol and 4-acetamidophenol, respectively. PANI$_n$–Fe efficiently and selectively catalysed acylation of benzylic hydroxyl and amines group in presence of phenolic group using acetic acid and no other oxidation products of phenols were observed (reaction condition: alcohol/amine (1.5 mmol), acetic acid 2 mL (39.21 mmol) and catalyst 25 mg at 100 °C). This is in contrast to the results obtained in the acylation of 2-aminophenol using acetic anhydride as acylating agent wherein both hydroxyl and amine groups were acylated when acylating agent was used in excess [20]. The comparative studies of acylation using PANI$_n$–Fe, PANI–Fe and FeCl$_3$ as a catalyst are also depicted in Fig. 7 to see the effectiveness of PANI$_n$–Fe catalyst under identical experimental conditions. Though
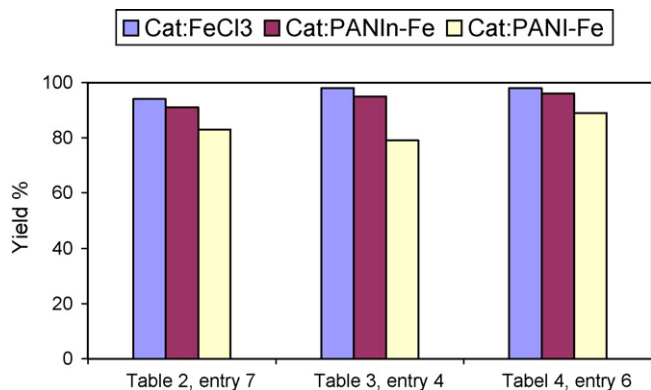
Fig. 7. Yields of acylated product using Cat: FeCl$_3$ (in homogeneous condition); using Cat: PANI$_n$–Fe; Cat: PANI–Fe [15].

We next planned to evaluate the efficiency of the PANI$_n$–Fe catalyst for acylation of amines (Scheme 2), a series of amines were subjected to acylation reaction and the results are summarized in Table 5. The reaction of aniline and substituted anilines with acetic acid gave the corresponding amides in excellent yields in shorter reaction times under solvent-free conditions (Table 5, entries 1–8). The presence of nitro group at *para* position of aniline and at *ortho*

Table 5
Acylation of amines with acetic acid using PANI$_n$–Fe[a].

Entry	Amines	Product	Time (h)	Isolated yield (%)
1	aniline (NH$_2$)	NHOAc	0.5	90
2	4-Cl-aniline	NHOAc	1.5	92
3	4-MeO-aniline	NHOAc	2.0	86
4	3-OMe-aniline	NHOAc	2.0	73
5	2-Me-aniline	NHOAc	2.0	21
6	4-F-aniline	NHOAc	1.0	96, 98[b], 89[c]
7	4-O$_2$N-aniline	NHOAc	2.5	41
8	2-NO$_2$-aniline	NHOAc	2.5	36
9	4-aminopyridine	NHOAc	4.0	69
10	cyclohexylamine	NHOAC	3.0	35
11	benzylamine	NHOAc	1.5	87
12	4-methylbenzylamine	NHOAc	0.5	47
13	4-MeO-benzylamine	NHOAc	2.0	86
14	phenethylamine	NHOAc	1.5	83
15	2,6-diethylaniline (Et)	NHOAc	4.0	–
16	2-aminophenol (OH)	NHOAc	0.5	45
17	4-aminophenol (HO)	NHOAc	0.5	86

[a] Amine 1.5 mmol, acetic acid 2 mL (39.21 mmol) and catalyst 25 mg at 100 °C.
[b] Yield using an FeCl$_3$ catalyst (162 mg, 1.0 mmol).
[c] Yield using PANI–Fe catalyst (50 mg).

Table 6
Recycling of PANI$_n$–Fe catalyst in acylation of 4-nitrobenzyl alcohol[a].

No. of cycles	Yield (%)[b]
Fresh	91
Run 1	91
Run 2	91
Run 3	91
Run 4	90
Run 5	90

[a] Reaction conditions: alcohol 0.229 g (1.5 mmol), acetic acid 2 mL (39.21 mmol) and catalyst 25 mg at 100 °C for 2 h.
[b] GC yields.

the Fe loading on the polyaniline nanofiber (PANI$_n$–Fe) and simple polyaniline (PANI–Fe) was same. i.e. ~5 wt.%, the yield of acylated product is higher with PANI$_n$–Fe. This might be due to the high content of Fe exposed on the surface of PANI$_n$ (polyaniline nanofiber has higher surface area and higher conductance) and thus with enhance Lewis acidic property. In homogeneous FeCl$_3$ catalysed reactions, though the catalyst activity was more compared to PANI$_n$–Fe and PANI–Fe, the loading of FeCl$_3$ was also high and it is non-recoverable and non-reusable catalyst. Thus FeCl$_3$ is inferior catalyst compared to PANI$_n$–Fe. FeCl$_3$·6H$_2$O is also active for the acylation reactions but it is not as efficient as FeCl$_3$, PANI$_n$–Fe and PANI–Fe because the presence of hydrate molecules affect the acidity of catalyst [21].

3.3. Reusability of the PANI$_n$–Fe catalyst

The recyclability and reusability of the PANI$_n$–Fe catalyst was tested for the acylation of 4-nitrobenzyl alcohol with acetic acid up to five cycles. The results are summarized in Table 6, showed that after every run, the yield of acylated product was unchanged, indicated the fair stability of PANI$_n$–Fe catalyst under experimental conditions. Whereas in case of PANI–Fe catalyst, considerable leaching was observed after two cycles only. This might be due to high conductivity of polyaniline nanofiber, which did not allow FeCl$_3$ to leach out from the system during catalytic reactions. The metal leaching of PANI$_n$–Fe and PANI–Fe catalyst was tested after every run by analyzing their respective reaction filtrates using atomic absorption spectroscopy. The salient features of this methodology are as: Tables 3–5 successfully demonstrated the esterification between acetic acid and several primary, secondary alcohols and amines smoothly in good to excellent yield in presence of PANI$_n$–Fe catalyst (5 wt.%); easy preparation, handling, stability and moisture insensitivity, easy recoverable and reusable makes the catalyst highly cost effective and environmentally acceptable; several functionalities in alcohols such as halogen, double bond, alicyclic and 4-nitrobenzyl were tolerated; in addition to several functionalities in amines, heterocyclic and cyclic amines were also tolerated; acylation of alcohol and amine in the presence of phenolic OH group was achieved selectively.

Regarding the mechanism, whether the reaction takes place by Lewis acid alone *via* intermediate **A** or Lewis acid assisted Brönsted acidity, the acylation of benzyl alcohol was studied using HCl-doped PANI and the reaction did not take place. In contrast, the corresponding PANI$_n$–Fe catalysed process afforded benzyl acetate selectively in 86%. These studies indicate that the present reaction may catalyse by Lewis acid as shown in Scheme 3 and not by Lewis acid assisted Brönsted acidity.

4. Conclusion

In summary, PANI$_n$–Fe was prepared, characterized and explored the utility for the acylation of diverse primary, secondary alcohols and amines with acetic acid to afford the corresponding acetates and acetamides in good to excellent yields. PANI$_n$–Fe catal-

ysed acylation offers several advantages; recyclability of the catalyst without loss of activity, ready availability and easy preparation of catalyst, has broad substrate applicability, with high product yields in short reaction time. The catalyst can be readily recovered and reused, thus making this process more environmentally acceptable.

Acknowledgements

References

[1] G. Cainelli, M. Contento, F. Manescalchi, L. Plessi, Synthesis (1989) 45.
[2] W.A. Herrmann, R.M. Kratzer, J. Blumel, H.B. Friedrich, R.W. Fischer, D.C. Apperley, J. Mink, O. Berkesi, J. Mol. Catal. A 120 (1997) 197–205.
[3] A. Severeyns, D.E. De Vos, L. Fiermans, F. Verpoort, P.J. Grobet, P.A. Jacobs, Angew. Chem. Int. Ed. 40 (2001) 586–589.
[4] R. Saladino, V. Neri, A.R. Pelliccia, R. Caminiti, C. Sadun, J. Org. Chem. 67 (2002) 1323–1332.
[5] S.V. Ley, C. Ramarao, A.-L. Lee, N. Ostergaard, S.C. Smith, I.M. Shirley, Org. Lett. 5 (2003) 185–187.
[6] S. Kobayashi, S. Nagayama, J. Am. Chem. Soc. 120 (1998) 2985–2986.
[7] S. Nagayama, M. Endo, S. Kobayashi, J. Org. Chem. 63 (1998) 6094–6095.
[8] S. Kobayashi, M. Endo, S. Nagayama, J. Am. Chem. Soc. 121 (1999) 11229–11230.
[9] R. Akiyama, S. Kobayashi, J. Am. Chem. Soc. 125 (2003) 3412–3413.
[10] M. Takeuchi, R. Akiyama, S. Kobayashi, J. Am. Chem. Soc. 127 (2005) 13096–13097.
[11] I.J. Bergeron, L.H. Dao, Macromolecules 25 (1992) 3332–3337.
[12] T. Nakajima, T. Kawagoe, Synth. Met. 28 (1989) C629–C632.
[13] T. Hirao, M. Higuchi, I. Ikeda, Y. Ohshiro, J. Chem. Soc. Chem. Commun. (1993) 194.
[14] M. Higuchi, D. Imoda, T. Hirao, Macromolecules 29 (1996) 8277–8279.
[15] E.N. Prabhakaran, J. Iqbal, J. Org. Chem. 64 (1999) 3339–3341.
[16] G. Kowalski, J. Pielichowski, Synlett (2002) 2107–2109.
[17] S. Velusamy, M. Ahmed, T. Punniyamurthy, Org. Lett. 6 (2004) 4821–4824.
[18] J. Izumi, I. Shiina, T. Mukaiyama, Chem. Lett. (1995) 141–142.
[19] A.K. Kumar, T.K. Chattopadhyay, Tetrahedron Lett. 28 (1987) 3713–3714.
[20] A.-X. Li, T.-S. Li, T.-H. Ding, Chem. Commun. (1997) 1389–1390.
[21] B.M. Choudary, V. Bhaskar, M. Lakshmi Kantam, K. Koteswara Rao, K.V. Raghavan, Green Chem. 2 (2000) 67–70.
[22] M. Akcay, Appl. Catal. A 269 (2004) 157–160, and reference there in.
[23] K. Jeeva Ratnam, R. Sudarshan Reddy, N.S. Sekhar, M. Lakshmi Kantam, F. Figueras, J. Mol. Catal. A: Chem. 276 (2007) 230–234.
[24] K.V.V. Krishna Mohan, N. Narender, S.J. Kulkarni, Green Chem. 8 (2006) 368–372.
[25] N. Narender, P. Srinivasu, S.J. Kulkarni, K.V. Raghavan, Synth. Commun. 30 (2000) 1887–1890.
[26] N. Narender, P. Srinivasu, S.J. Kulkarni, K.V. Raghavan, Green Chem. 3 (2003) 104–105.
[27] S.-g. Lee, J.H. Park, J. Mol. Catal. A: Chem. 194 (2003) 49–52.
[28] S. Bogaert, T. Chenal, A. Mortreux, J. Carpentier, J. Mol. Catal. A: Chem. 181 (2002) 207–214.
[29] S. Joy, Dissertation work, Master of Biotechnology.
[30] F. Shirini, M.A. Zolfigol, M. Abedini, P. Salehi, Bull. Korean Chem. Soc. 24 (2003) 1683–1685.
[31] B. Sreedhar, V. Bhaskar, Ch. Sridhar, T. Srinivas, J. Mol. Catal. A: Chem. 191 (2003) 141–147.
[32] F. Genoud, I. Kulszewicz-Bajer, A. Bedel, J. Louis Oddou, C. Jeandey, A. Pron, Chem. Mater. 12 (2000) 744–749.
[33] O.P. Dimitriev, Macromolecules 37 (2004) 3388–3395.
[34] J.F. Moulder, W.F. Stickle, P.E. Sobol, K.D. Bomden, Handbook of X-ray Photoelectron Spectroscopy, Perkin–Elmer Corp., 1992.
[35] B.-J. Kim, S.-G. Oh, M.-G. Han, S.-S. Im, Langmuir 16 (2000) 5841–5845.
[36] M. Harada, M. Adachi, Adv. Mater. 12 (2000) 839–841.
[37] CRC Handbook of Chemistry and Physics, 61st ed., in: R.C. Weast, M.J. Astle (eds.), CRC Press, Inc., Boca Raton, FL, 1980–1981, pp. D-155–D-160.
[38] K. Ishihara, M. Nakayama, S. Ohara, H. Yamamoto, Synlett (2001) 1117–1120.
[39] M. Nakayama, A. Sato, K. Ishihara, H. Yamamoto, Adv. Synth. Catal. 346 (2004) 1275–1279.
[40] C.T. Maki, K. Ishihara, H. Yamamoto, Org. Lett. 7 (2005) 5047–5050.
[41] D.K. Ishihara, S. Nakagawa, A. Sakakura, J. Am. Chem. Soc. 127 (2005) 4168–4169.
[42] E.T. Funatomi, K. Wakasugi, T. Misaki, Y. Tanabe, Green Chem. 8 (2006) 1022–1027.
[43] F.H. Firouzabadi, N. Iranpoor, S. Farahi, J. Mol. Catal. A: Chem. 289 (2008) 61–68.